Current ramps in tokamaks : from present experiments to ITER scenarios

F. Imbeaux[1], V. Basiuk[1], R. Budny[2], T. Casper[3], J. Citrin[4], J. Fereira[5], A. Fukuyama[6], J. Garcia[1], Y.V. Gribov[3], N. Hayashi[7], J. Hobirk[8], G.M.D. Hogeweij[4], M. Honda[7], I. H. Hutchinson[9], G. Jackson[10], A.A. Kavin[11], C. E. Kessel[2], R.R. Khayrutdinov[12], F. Köchl[13], C. Labate[14], V. M. Leonov[12], X. Litaudon[1], P.J. Lomas[15], J. Lönnroth[16], T. Luce[10], V.E. Lukash[12], M. Mattei[17], D. Mikkelsen[2], S. Miyamoto[7], Y. Nakamura[18], I. Nunes[5], V. Parail[15], G. Pereverzev[8], Y. Peysson[1], A. Polevoi[3], P. Politzer[10], M. Schneider[1], G. Sips[19], G. Tardini[8], I. Voitsekhovitch[15], S. M. Wolfe[9], V.E. Zhogolev[12], ASDEX Upgrade Team, C-Mod Team, DIII-D Team, JET-EFDA contributors[*], JT-60U Team, Tore Supra Team, contributors of the EU-ITM ITER Scenario Modelling group, ITPA "Integrated Operation Scenarios" group members and experts and ITPA "Transport and Confinement" group members and experts

1. CEA, IRFM, F-13108 Saint Paul Lez Durance, France
2. Princeton Plasma Physics Laboratory, P.O. Box 451, Princeton, NJ USA
3. ITER Organization, Route de Vinon sur Verdon, F-13115 St Paul lez Durance, France
4. FOM Institute for Plasma Physics Rijnhuizen, Association EURATOM-FOM, Nieuwegein, The Netherlands
5. Association Euratom-IST, Lisboa, Portugal
6. Kyoto University, Sakyo-ku, Kyoto, 606-8501 Japan
7. Japan Atomic Energy Agency, 801-1, Mukouyama, Naka, Ibaraki-ken 311-0193, Japan
8. Max-Planck-Institut für Plasmaphysik, EURATOM-Assoziation, Garching, Germany
9. Plasma Science and Fusion Center, MIT, Cambridge, MA USA
10. General Atomics, San Diego, USA
11. NIIEFA, St. Petersburg, Russia
12. RRC "Kurchatov Institute", Moscow, Russia
13. Association EURATOM-ÖAW/ATI, Vienna, Austria
14. Associazione ENEA/CREATE, DIMET, Università di Reggio Calabria Via Graziella, 89100, Calabria, Italy
15. EURATOM/CCFE Fusion Association, Culham Science Centre, Abingdon OX14 3DB UK
16. Association EURATOM-TEKES, Helsinki University of Technology, Finland
17. Associazione ENEA/CREATE, DIAM, Seconda Università di Napoli Via Roma 29, 81031, Aversa, Italy
18. Nippon Advanced Technology Co., Ltd. Tokai, Ibaraki 319-1112 Japan
19. EFDA CSU, JET, UK

e-mail: *frederic.imbeaux@cea.fr*

Abstract. In order to prepare adequate current ramp-up and ramp-down scenarios for ITER, present experiments from various tokamaks have been analysed by means of integrated modelling in view of determining relevant heat transport models for these operation phases. The most accurate heat transport models are then applied to projections to ITER current ramp-up, focusing on the baseline inductive scenario (main heating plateau current of Ip = 15 MA). These projections include a sensitivity studies to various assumptions of the simulation. While the heat transport model is at the heart of such simulations (because of the intrinsic dependence of the plasma resistivity on electron temperature), more comprehensive simulations are required to test all operational aspects of the current ramp-up and ramp-down phases of ITER scenarios. Recent examples of such simulations, involving coupled core transport codes, free boundary equilibrium solvers and a poloidal field (PF) systems controller are described in the second part of the paper, focusing on ITER current ramp-down.

1 Introduction

The scenario design of a future tokamak device naturally focuses on the main heating phase, where fusion reactions take place. Nevertheless, the conditions to access, and eventually to terminate smoothly, the desired main heating state is also an essential topic. The main heating phase is usually carried out at high plasma current, since in a tokamak high current means high confinement. This current is ramped up from a negligible value just after the plasma breakdown to a plateau value, usually mainly by inductive means. After the main heating phase, the plasma current and energy content must also be ramped down smoothly before

[*] See the Appendix of F. Romanelli et al., paper OV/1-3, this conference

stopping the plasma discharge. There are several issues to be addressed during plasma current ramp phases of tokamak operation: Magnetohydrodynamic (MHD) activity can take place and lead to early plasma termination, depending on the shape of the plasma current density profile. The design of the Poloidal Field (PF) system and plasma shape controller must allow ramping up the plasma current while providing stable plasma equilibrium. In addition, a significant amount of magnetic flux is needed to ramp the plasma up inductively, thus the flux consumption during the current ramp is also a key element in the design of the PF system. Finally, the confinement / MHD properties of the final "main heating" phase depend on the q-profile obtained at the end of the ramp-up and may be optimised by applying additional heating and non-inductive current drive during the current ramp.
Current ramp down in ITER is also quite a challenging part of plasma operation. Apart from the issue of not exceeding the density limit, a burning plasma is usually in H mode before the current ramp-down and shall return to L-mode before termination. During the H-L transition the plasma quickly loses energy content, which needs to be properly handled by the vertical stability system.
In order to prepare adequate current ramp-up and ramp-down scenarios for ITER, present experiments from various tokamaks (mainly JET, and also ASDEX Upgrade, Tore Supra) have been analysed by means of integrated modelling in view of determining heat transport models relevant for the current ramp-up and ramp-down phases. The results of these studies are presented and projections to ITER current ramp-up and ramp-down scenarios are done, focusing on the baseline inductive scenario (main heating plateau current of Ip = 15 MA).
While the heat transport model is at the heart of such simulations (because of the intrinsic dependence of the plasma resistivity on electron temperature), more comprehensive simulations are required to test all operational aspects of the current ramp-up and ramp-down phases of ITER scenarios. Recent examples of such simulations, involving coupled core transport codes, free boundary equilibrium solvers and a PF systems controller are described in the second part of the paper (section 3).

2 Heat transport studies for current ramp-up

We present here simulations aiming at validating heat transport models on existing experiments, then use the validated models for extrapolation to ITER. The simulations reported in this section are solving the one-dimensional (radial direction) fluid transport equations on poloidal magnetic flux (current diffusion equation) and electron and ion heat transport. The equilibrium is calculated consistently with the results of the transport equations, using fixed boundary solvers. When analysing present experiments, the shape of the Last Closed Flux Surface (LCFS) prescribed in the simulation is determined from magnetic measurements.

2.1 Validating heat transport models against present current ramp-up experiments

A database of 8 discharges, mainly from the JET tokamak, has been selected covering ohmic current ramp-up cases, as well as ramp-up assisted with moderate additional heating (up to a few MW). While JET dominates the dataset, a few experiments from Tore Supra and ASDEX Upgrade have been used as well, in order to test the validity of the models for different machine size and plasma shape, which is quite important in view of extrapolation to ITER. Up to now, this heat transport model validation effort has essentially been conducted by modellers from the Iter Scenario Modelling group of the European Integrated Tokamak Modelling Task Force (see [1] for a presentation of the first results of this group), using the three major European transport codes, namely ASTRA [2], CRONOS [3] and JETTO [4]. This has been the occasion of detailed code benchmarking, quite useful to detect possible

mistakes in simulation parameterization and numerical problems, as well as to verify the details of the implementation of the transport models.
The current diffusion and heat transport equations for the electron and ion channels are solved consistently. The electron density profile is prescribed from measurements (Abel inversion of line-integrated interferometer measurements). Flat *Zeff* profile is assumed, with a uniform value of *Zeff* prescribed from Bremsstrahlung measurements. We also prescribe the radiated power profile from Abel inversion of bolometry measurements, when available. Toroidal rotation is not taken into account. As no or moderate NBI power was used plasma rotation is expected to be low and have negligible impact on heat transport.
The internal inductance $li(3) = \frac{2V\left\langle B_P^2 \right\rangle}{(\mu_0 I_P)^2 R_0}$ has been chosen as essential parameter / criterion for validation of the heat transport models in the context of current ramp-up and ramp-down phases (where V is the plasma volume, I_p the plasma current, R_0 the major radius of the plasma and $\langle\ \rangle$ denotes average over the whole plasma volume : $\left\langle B_P^2 \right\rangle = 1/V \int B_P^2 dV$). This parameter is important from the operational point of view since i) the range of current profile shapes that can be sustained by the Poloidal Field coils can be characterised by an interval of *li*; ii) *li* is a key parameter for the vertical instability; iii) *li* is also a key parameter for typical Magneto-Hydrodynamical (MHD) activity during the ramp-up.
Being a normalised volume averaged quantity, the internal inductance is strongly weighted by the outer half of the plasma. Therefore details of the current density profile inside mid-radius have a weak impact on the *li* value. The prediction of *li* dynamics depends essentially on the electron temperature profile outside mid-radius. Even if the heat transport model deviates from the *Te* measurements inside mid-radius, or is not accurate on the ion temperature prediction, it may be judged relevant for the prediction of this key operational parameter.
The models tested are the following :

- Scaling-based models, using a fixed radial shape $\chi(\rho,t) = A(t)(1+6\ \rho^2 + 80\ \rho^{20})$. The time-dependent factor A(t) is adjusted at each call of the model in order that the plasma thermal energy content W_{th} follows a known scaling expression, namely: $W_{th} = H\tau_E\left(P_{loss} - \dot{W}_{th}\right)$. Two scaling expressions for the energy confinement time τ_E have been used : the ITER96-L (L-mode) [5] scaling and the IPB98 (H-mode) scaling [6]. The optimal agreement between experiment and simulations (using *li* and flux consumption as criterion) with this model in our current ramp-up dataset is obtained using either $H_{96\text{-}L} = 0.6$ or $H_{IPB98} = 0.4$. Interestingly, the energy confinement time during current ramp-up phases of selected DIII-D and C-MOD discharges (not included in the validation dataset yet) follow approximately the same *H* factors, which strengthens the confidence in this scaling-based approach.
- The empirical Bohm/gyro-Bohm model, in its original L-mode version without magnetic shear dependence [7].
- The Coppi-Tang model [8]
- The GLF23 model [9]

Figures 1-2 present some typical highlights of this comparison of the models to experimental data, which includes both ohmic and discharges with moderate heating during the current ramp-up. In these figures, like in our dataset in general, all models reproduce the *li* dynamics within +/- 0.15. On the JET discharge #71827 the B/gB and GLF23 models are most accurate in Te and li while the scaling-based models tend to overestimate Te in the core. However this behaviour is not general, for the Tore Supra case (Fig. 2) the scaling-based models are the most accurate in terms of electron temperature. As a consequence they are also the most accurate for correlating the time of occurrence of the first sawtooth in experiment and the

occurrence of the q = 1 surface in the simulations (see Table 1). The AUG discharge in our dataset is not reproduced as well by the models so far. The reason is most probably that the outer third of this discharge is impurity dominated (unboronised machine) and a careful treatment of the radiated power must be applied in the simulation. From the JET case (Fig. 1), the Coppi-Tang model grossly overestimates the electron temperature and li. Using the first-principle based GLF23 model in the current ramp-up phases is a challenge, in particular because our figure of merit is strongly weighted by what happens in the outer half of the plasma. When applied up to the LCFS, the GLF23 model tends to predict very low level of transport resulting in a sort of pedestal in *Te*, which is not consistent with the experimental data and leads to a strong underestimation of li. This behaviour seems to be general on our dataset. In order to correct this problem, the model has been arbitrarily patched in the region $0.8 < \rho < 1$ by prescribing a fixed diffusion coefficient $\chi_e = \chi_i = 8$ m^2/s. With this patch, GLF23 provides rather accurate li and Te dynamics on the JET shots, though still has problems reproducing the *Te* profile on Tore Supra. The Bohm/gyro-Bohm and scaling-based models remain the most satisfying ones, yielding on our dataset (but the AUG impurity dominated discharge) the correct li dynamics within +/- 0.15.

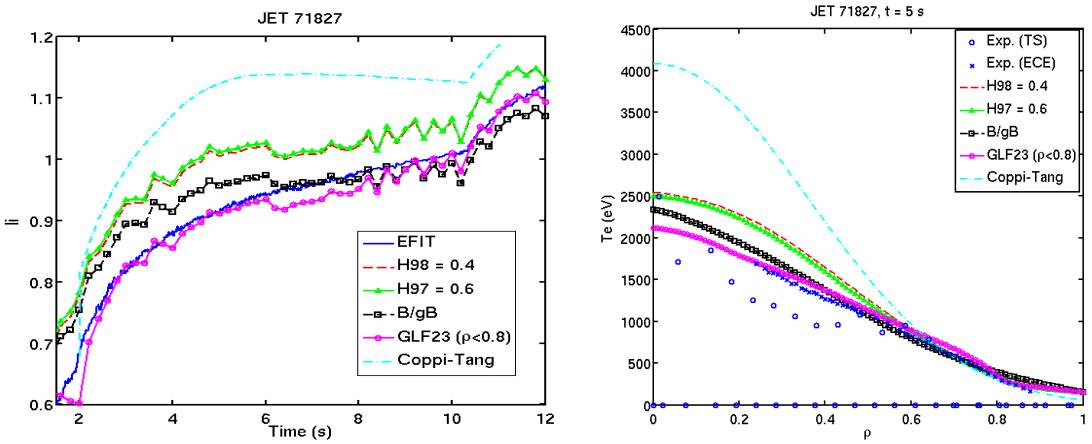

Figure 1 : Left : Simulation of the internal inductance dynamics of a JET ohmic shot with several heat transport models. The plasma current is ramped up to 2.5 MA in 10 s. Experimental value (EFIT reconstruction, blue), scaling-based (H_{98} = 0.4, red dash), scaling-based (H_L = 0.6, green triangles), Bohm/gyro-Bohm (black squares), GLF23 (applied only inside ρ = 0.8 with $\chi_e = \chi_i = 8$ m^2/s outside, purple), Coppi-Tang (light blue dash dotted). Right : Electron temperature profile at t = 5 s. Blue circles and crosses indicate experimental measurements (Thomson Scattering and Electron Cyclotron Emission respectively), the other profiles correspond to the models predictions, same colour code as at left.

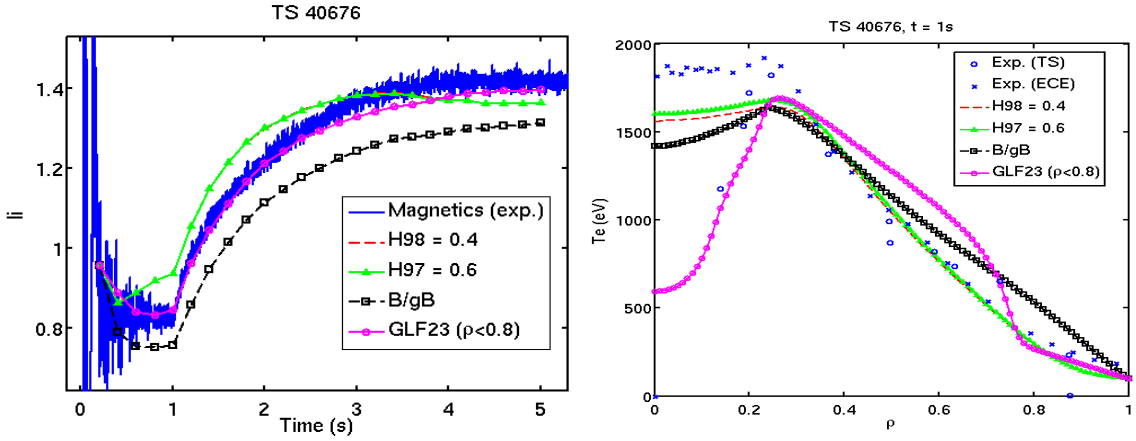

Figure 2 : Left : Simulation of the internal inductance dynamics of a Tore Supra ECCD assisted current ramp-up (500 kW co-ECCD applied at ρ = 0.3 from t = 0.4 s onwards) with several heat transport models. The plasma current is ramped up to 0.9 MA in 1 s. Same colour code as Fig. 1. Right : Electron temperature profile at t = 1 s.

	Exp.	BgB	GLF23	Scaling H98=0.4	Scaling H97=0.6
t(q = 1) [s]	2.4	3	2.8	2.2	2.4

Table 1: Tore Supra shot #40676. Time of occurrence of the first sawtooth in experiment (2st column) and of occurrence of the q = 1 surface in the simulations with various models.

2.2 Projections to ITER

Using the most accurate transport models, projections to the ITER current ramp-up phase are carried out. In Figure 3, the electron temperature and safety factor profiles at the end of the current ramp-up (ITER inductive scenario) are displayed, in the case where 20 MW of ECRH are added at mid-radius early in the ramp. Though significant differences between models appear on the electron temperature prediction (in particular inside the ECRH deposition), the final q-profiles reached in the simulation are rather close. The difference between models on the li(3) prediction is also small, of the same order as for the present experiments, i.e. +/- 0.1. Thus, even in an ITER case with strong and narrow heating source, all selected transport models behave rather similarly in terms of li dynamics and target q-profile, providing a prediction envelope which, for the experimental validation dataset was containing the experimental value.

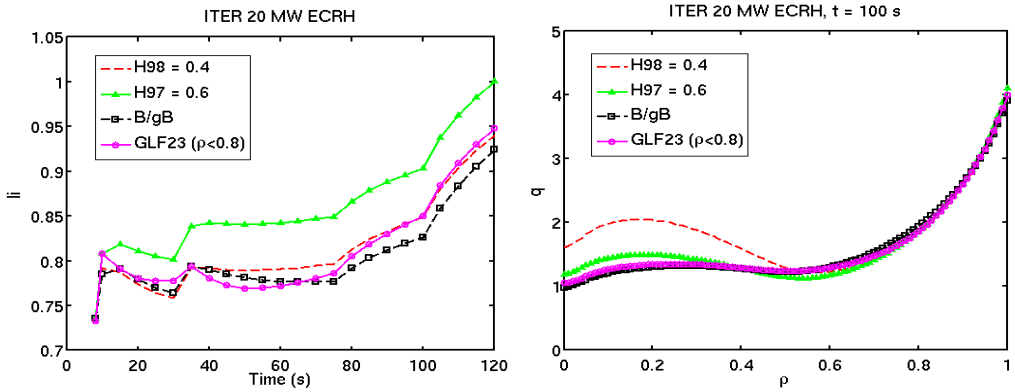

Figure 3 : Projection of the ITER current ramp-up phase in case 20 MW of ECRH are added at mi-radius early in the ramp (flat-top value Ip = 15 MA reached at t = 100 s). The most accurate heat transport models have been used : scaling-based (H_{98} = 0.4, red dash), scaling-based (H_L = 0.6, green triangles), Bohm/gyro-Bohm (black squares), GLF23 (applied only inside ρ = 0.8 with $\chi_e = \chi_i$ = 8 m^2/s outside, purple). Left: dynamics of the internal inductance. Right : q-profile at the end of the current ramp.

In this case with additional heating during the current ramp-up, all models yield a target q-profile where q > 1 on the whole radius, ideal for e.g. a hybrid scenario. Note that this occurs even if none of the empirical models used here accounts for Internal Transport Barrier (ITB) (the model GLF23 potentially takes ITBs into account but does not trigger one here). When using the CDBM model, which well reproduces a JT-60U reversed-shear discharge [10], ECCD applied at mid-radius during the ITER current ramp-up triggers an ITB, delaying the current penetration inside mid-radius and yielding a strongly reversed target q-profile (Fig. 4).

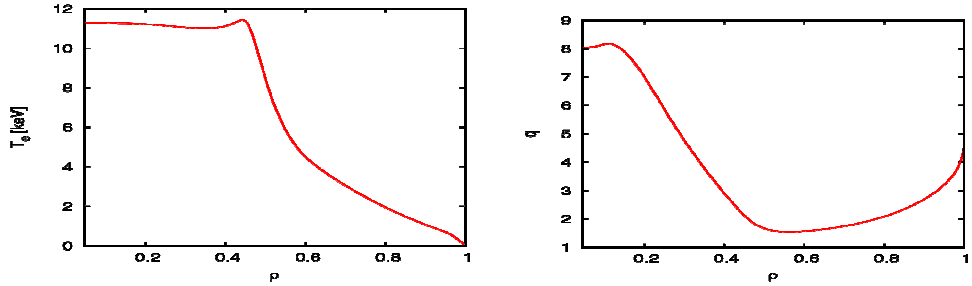

Figure 4 : Projection of the ITER current ramp-up phase in case 20 MW of ECRH are added at mid-radius early from t = 10 s onwards (flat-top value Ip = 15 MA reached at t = 70 s). The dynamic evolution of plasma expansion is solved by the TSC code with the CDBM transport model. Electron temperature (left) and q-profile (right) at the end of the current ramp.

Those projections are documented with sensitivity analysis. Indeed the absolute value of li and its dynamics depend on physical parameters that are given when analyzing present experiments but which have to be assumed in case of projection to ITER. These are: effective charge, initial conditions, boundary conditions for the transport equations, plasma shape and last but not least electron density. Figure 5 presents such a sensitivity analysis on *Te* boundary condition *Tea* and *Zeff* dynamics in the case of an ohmic ITER ramp-up. The impact of the *Tea* variation is relatively small (less than 0.05 in li at the end of the Ip ramp-up), while using high Zeff at the beginning of the current ramp-up makes a quite strong difference in li during the early phase, which eventually disappears at the end of the ramp-up.

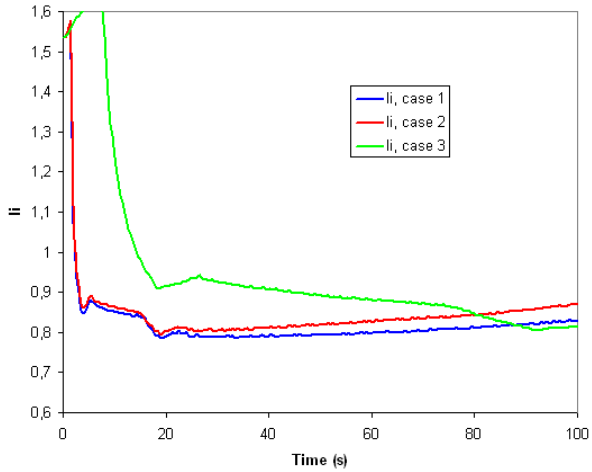

Figure 5: Sensitivity analysis in case of an ohmic ITER ramp-up case (flat-top value 15 MA reached at t = 100 s) with the scaling-based model H_{98} = 0.4. Case 1 (blue): constant Zeff = 1.7, Tea ramped up from 25 to 250 eV. Case 2 (red): constant Zeff, Tea 25-100 eV. Case 3 (green): Zeff ramped down from 4 to 1.7, Tea 25-250 eV.

3 Integrated Simulations of ITER current ramp-down

Figure 6 illustrates two possible ITER fast current ramp-down scenarios, simulated by the Astra code [11], one with an H-L back transition (left), the other maintaining the plasma in H-mode with the use of higher heating power (right). The main challenge with the H-L back transition is the sudden drop of pressure (see β_P on the figure), which may cause a significant inward shift of the plasma and contact to the wall. Conversely the scenario of plasma termination in H-mode has no significant drop of β_P, but features a large increase of li at the end of the discharge which could cause vertical instability when I_P reaches 3 MA.

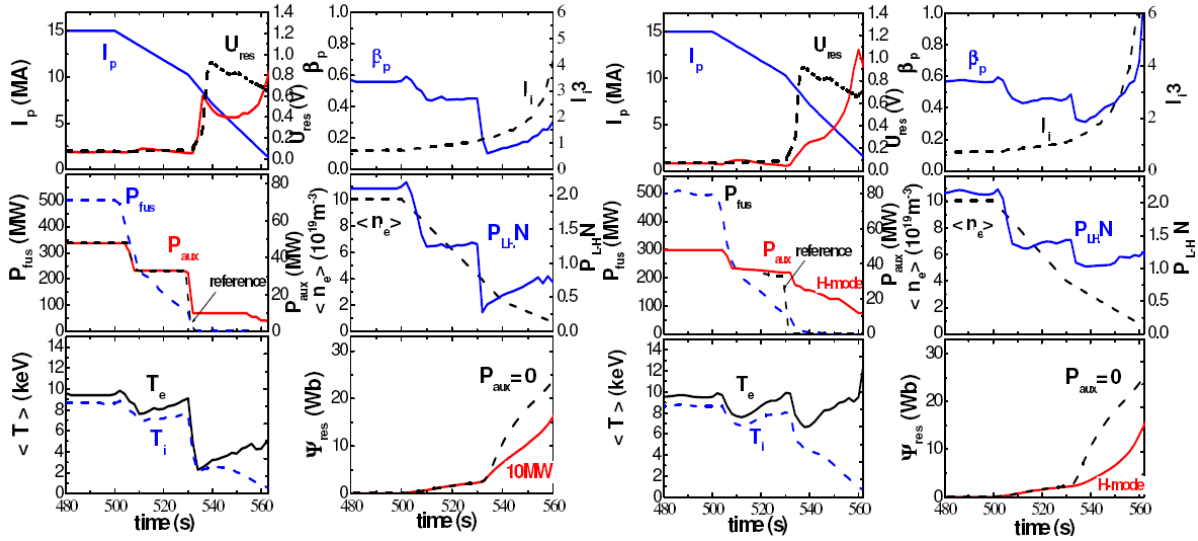

Figure 6: Plasma termination scenarios in L-mode (left), and in H-mode (right), simulated with the Astra code.

The fact that the plasma energy content changes so rapidly after the H-L transition points to the importance of a self-consistent simulation of plasma equilibrium using free boundary equilibrium solvers, together with the core transport equations and PF systems controller. Figure 7 shows one example of such a simulation carried out with JETTO and CREATE-NL, which was applied to an

extract from Scenario-2 plasma containing both L-H and H-L transitions. Although the presently adopted ITER shape control system can cope with both L-H and H-L transitions, the latter can push plasma onto the inner limiter when the plasma energy content exceeds level of W_{th}>35MJ. Successful self-consistent simulation of ITER current ramp-down scenario with DINA-CH coupled to the CRONOS Integrated Modelling code can be found in [12].

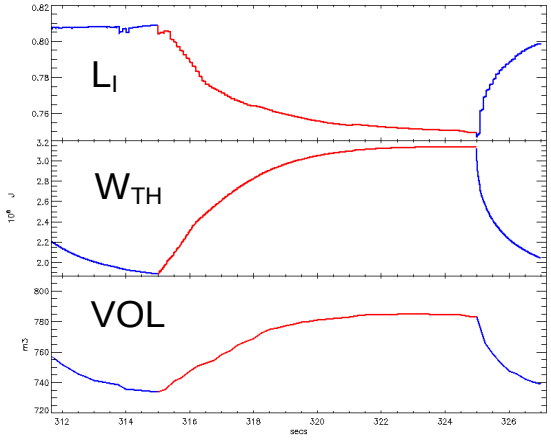

Figure 7. From top to bottom: internal inductance (plasma is in L-mode when colour is blue and in H-mode when colour is red), plasma thermal energy content and plasma volume

Together with the plasma current, the plasma density must also be ramp-down without causing excessive divertor power load and while controlling divertor detachment. Using a simple model of edge/core fuelling control, TSC simulations of the ramp-down from ITER burning flat-top were performed on ITER 15MA/200s termination scenario. The TSC, comprised of two-dimensional free boundary plasma equilibria and one-dimensional transport model (CDBM), describes time-evolution of the plasma shape and profile dynamics of the plasma current Ip and temperature as well as density. The plasma density was controlled by feedback on neutral gas puff from the edge and core fuelling like pellet injection. Two ramp-down scenarios have been studied, one keeping the edge/core fuelling control invariant ($f_{edge/core}$ = 0.8, Figure 8 left), in the other $f_{edge/core}$ is ramped down linearly from 0.8 at 500 sec to 0.0 (totally core fuelling) at t = 600 s (Figure 8 right). Time-evolution of divertor neutral pressure p0 was solved by 0-dimensional model of coming and going of plasma particle, accumulation and pumping-out dynamics of fuelling gas. The H-L mode transition was forced at 600 sec. Figure 8 shows the dynamics of some of the SOL/divertor parameters, which are quite different depending on the fuelling scenario. It thus follows that edge/core fuelling control during the termination of ITER discharge is a key operating instruction for a slow and safe density ramp-down from high-Q burning flat-top.

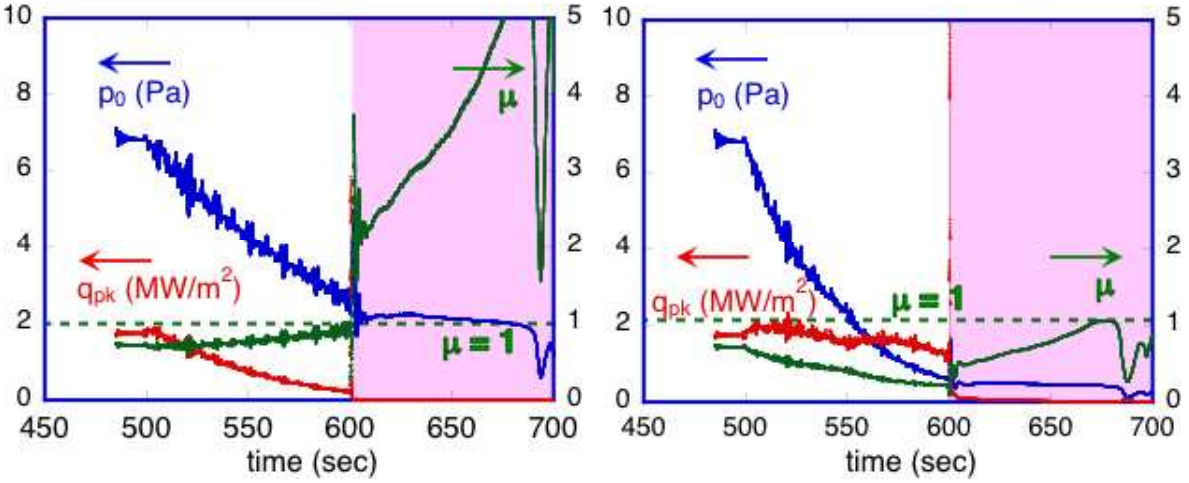

Figure 8: Left : Simulation of the divertor power load q_{pk}, the normalized neutral pressure μ and the divertor neutral pressure p_0, keeping the edge/core fuelling control invariant ($f_{edge/core}$ = 0.8). Right after H-L transition at 600 sec, the operating point of inner divertor becomes strongly detached (μ >> 1). Right : Simulation of q_{pk}, μ and p_0, changing $f_{edge/core}$ from 0.8 at 500 sec to 0.0 (totally core fuelling) at 600 sec. Even after H-L transition, the operating point of inner divertor remains attached in "regime A" (μ < 1), though a higher heat pulse more than 10 MW/m^2 arises at the H-L transition.

4 Conclusions

During the past two years, significant modelling efforts have been carried out throughout the world to simulate the current ramp up and ramp down phases of the 15 MA ITER reference scenario. In particular, a set of empirical heat transport models for L-mode has been validated on existing experiments for predicting the li dynamics within +/- 0.15 accuracy during current ramp-up and ramp-down phases. This accuracy is obtained using the density profile peaking and the electron temperature boundary condition (at the LCFS) from the experiment, which of course is not possible for present extrapolations to ITER. Therefore the sensitivity of the predictions using these models has been quantified when applied to ITER current ramp-up simulations. While the heat transport model is at the heart of such simulations (because of the intrinsic dependence of the plasma resistivity on electron temperature), more comprehensive simulations are required to test all operational aspects of the current ramp-up and ramp-down phases of ITER scenarios. These simulations should involve coupled free-boundary equilibrium solvers, core transport code and PF systems circuit equations including voltage controller, in order to test the capability of the ITER PF systems to handle the chosen scenario. The H-L back transition at the end of the burn is one of the challenging phases of the operation that must be prepared by such complex integrated simulations. Another challenging aspect is the modelling of the plasma breakdown, which sets the initial conditions prior to the current ramp-up. This should also be addressed in the future, likely with dedicated codes and models for describing the specific processes occurring during this phase (pre-ionization, burnthrough, …). Another key ingredient that should be integrated in the simulations is particle fuelling and transport, including core edge interaction in order i) to verify that the chosen scenario can be indeed fuelled and ii) to check the operational limits of the divertor. This work shows recent examples of such highly integrated simulations, which presently are far from routine usage. In the recent years, modeling codes have progressed technically to reach this high level of integration of the usual core transport equations with more and more operational aspects. Nonetheless, a strong effort of validation of the individual models used in these integrated simulations on existing experiments remains the backbone and starting point of any extrapolation procedure and a significant effort has still to be carried out in this area. Dedicated scaled experiments are interesting for this purpose [13]. Ultimately, the developed models and integrated simulators will provide an essential support to the preparation of ITER scenarios and operation.

Acknowledgements

This work was partly supported by EURATOM and carried out within the framework of the European Fusion Development Agreement. The views and opinions expressed herein do not necessarily reflect those of the European Commission. The views and opinions expressed herein do not necessarily reflect those of the ITER Organization.

References

[1] Parail V., Belo P., Boerner P., Bonnin X. et al 2009 Nucl. Fusion **49** 075030
[2] Pereverzev G.V., Yushmanov P.N., Report IPP 5/98 (2002), Garching
[3] Artaud J.F., Basiuk V., Imbeaux F., Schneider M. et al 2010 Nucl. Fusion **50** 043001
[4] Cennacchi G. and Taroni A., Report JET-IR(88) 03
[5] Kaye S et al. 1997, Nucl. Fusion **37** 1303
[6] ITER Physics Basis 1999 Nucl. Fusion **39** 2137
[7] Erba M., Aniel T., Basiuk V. Becoulet A. and Litaudon X. 1998 Nucl. Fusion **38** 1013
[8] Jardin S.C. , Bell M.G. and Pomphrey N. 1993 Nucl. Fusion **33** 371
[9] Waltz R.E., Staebler G. M., Dorland W. 1997, Hammett G. W. et al, Phys. Plasmas **4** 2482
[10] Takei N., Nakamura Y., et. al. 2007, Plasma Physics and Controlled Fusion **49** 335
[11] Leonov M. et al 2010, 37th EPS Conf. on Plasma Physics and Controlled Fusion (Dublin, Ireland) P-2.182
[12] Kim S.H., Artaud J.F., Basiuk V., Dokuka V. et al 2009, Plasma Phys. Control. Fusion **51** 105007, and this Conference THW/P2-02
[13] Jackson G.L., Politzer P.A., Humphreys D.A., Casper T.A. et al 2010 Phys. Plasmas **17** 056116